Tuba, a Cdc42 GEF, is required for polarized spindle orientation during epithelial cyst formation

Yi Qin,[1,2] Walter H. Meisen,[1,2] Yi Hao,[1,2] and Ian G. Macara[1,2]

[1]Center for Cell Signaling and [2]Department of Microbiology, University of Virginia School of Medicine, Charlottesville, VA 22908

The Cdc42 guanosine triphosphatase is essential for cell polarization in several organisms and in vitro for the organization of polarized epithelial cysts. A long-standing question concerns the identity of the guanine nucleotide exchange factor (GEF) that controls this process. Using Madin–Darby canine kidney cells grown in Matrigel, we screened 70 GEFs by RNA interference. Of these, six positives were identified that caused a multilumen phenotype, including Tuba, a Cdc42-specific GEF localized below the apical cortex. Loss of Tuba abolishes Cdc42 enrichment at the apical cortex. Normal lumen formation is rescued by human Tuba or active Cdc42 but not by a GEF-negative Tuba mutant. Silencing Cdc42 causes a similar phenotype, including multilumen formation and reduced atypical protein kinase C (aPKC) activity. Lumen disorganization after depletion of Tuba or Cdc42 or inhibition of aPKC is caused by defective spindle orientation. Together, our findings implicate Tuba as a key activator of the Cdc42 GTPase during epithelial ductal morphogenesis, which in turn activates apical aPKC to ensure that spindles orient parallel to the lateral plane.

Introduction

The Cdc42 GTPase is an ancient, highly conserved polarity protein that was discovered in the budding yeast *Saccharomyces cerevisiae*, where it plays a key role in bud site establishment (Casamayor and Snyder, 2002). It has since been implicated in epithelial cell polarization in several organisms (Hutterer et al., 2004; Wu et al., 2007; Anderson et al., 2008) and is required in vitro for the organization of polarized epithelial cysts (Martín-Belmonte et al., 2007). A long-standing question concerns the identity of the upstream activator or activators of Cdc42 that control this process. In eukaryotes, Cdc42 can interact with a heterodimer of the polarity proteins Par6 and atypical PKC (aPKC; Joberty et al., 2000; Lin et al., 2000; Garrard et al., 2003) and is important for polarization in a variety of contexts. Cdc42 belongs to the Rho family of small GTPases and functions as a molecular switch. Guanine nucleotide exchange factors (GEFs) and GTPase-activating proteins (GAPs) catalyze conversion between the GTP- and GDP-bound forms. Generally, the GTP-bound forms associate with effector proteins that participate in a variety of signaling pathways. Cdc42-GTP binding to Par6 relieves an inhibitory constraint on aPKC (Yamanaka et al., 2001; Atwood et al., 2007). Cdc42 can also recruit Par6 to specific locations within the cell that are enriched for the GTP-bound form (Hutterer et al., 2004; Atwood et al., 2007). Therefore, Cdc42 might promote the phosphorylation of aPKC targets in a spatially discrete manner.

In *Caenorhabditis elegans*, the interaction of Cdc42 with Par6 is essential for maintenance of polarity and asymmetric cell division of the zygote (Aceto et al., 2006; Motegi and Sugimoto, 2006), and they function together in a diversity of cell types during nematode development (Welchman et al., 2007). Cdc42 helps recruit Par6 to the cell cortex (Schonegg and Hyman, 2006). After the initial cell divisions of the zygote, Par6 is limited to outward-facing membranes that are not in contact with other cells, and this restriction depends on the complementary localization of a Cdc42 GAP to the cell–cell contacts (Anderson et al., 2008). Therefore, spatially localized hydrolysis of Cdc42-GTP helps define polarity by excluding Par6 from cell–cell contacts. Whether there is local activation of Cdc42 by a GEF remains to be determined.

Correspondence to Ian G. Macara: igm9c@virginia.edu

Abbreviations used in this paper: aPKC, atypical PKC; GAP, GTPase-activating protein; GEF, guanine nucleotide exchange factor; hTuba, human Tuba; shRNA, short hairpin RNA.

The Rockefeller University Press $30.00
J. Cell Biol. Vol. 189 No. 4 661–669
www.jcb.org/cgi/doi/10.1083/jcb.201002097

Cdc42 is also required for Par6 localization in *Drosophila melanogaster* embryos. Loss of Cdc42 from embryonic neuroblasts (Atwood et al., 2007) and epithelial cells (Hutterer et al., 2004) prevents recruitment of Par6–aPKC to the apical cortex and disrupts polarity, and the GTP-bound form of Cdc42 mediates Par6 recruitment. Another polarity protein, Lgl, excludes Par6 from the basolateral cortex (Hutterer et al., 2004), but it is not known if it also excludes Cdc42-GTP. The mechanism by which Cdc42 is activated at the apical cortex is also not understood.

The role of Cdc42 in mammalian cell polarity has been studied extensively in epithelial cells and migrating astrocytes (Etienne-Manneville and Hall, 2001; Martín-Belmonte et al., 2007). Cdc42 is essential for spindle orientation and normal cyst morphogenesis in 3D cultures of Caco-2 epithelial cells (Jaffe et al., 2008). In turn, Cdc42 targets Par6–aPKC to the apical cortex (Martín-Belmonte et al., 2007). Cdc42 also localizes to the leading edge of migrating astrocytes and may be required to recruit the Par6–aPKC complex (Etienne-Manneville and Hall, 2001). A Cdc42-specific GAP, Rich1, has been implicated in junction assembly between epithelial cells (Wells et al., 2006), but no GEFs have yet been tied to epithelial cell polarization or oriented migration. Therefore, a key question is how Cdc42 becomes activated during cell polarization. Possible models include a localized GEF that produces Cdc42-GTP at spatially discrete sites or a diffusely distributed GEF plus a localized GAP that depletes Cdc42-GTP from reciprocal regions of the cell, or some combination of these two mechanisms.

To address this central question, we created a short hairpin RNA (shRNA) library that targets all known canine Rho family GEFs and tested the ability of these shRNAs to disrupt lumen formation in MDCK epithelial cysts grown in Matrigel cultures. We identified several GEFs that are required for normal lumen formation, including one called Tuba, which is specific for Cdc42. We show that the GEF activity of Tuba is required for correct spindle pole orientation during cyst formation, a process mediated through activation of aPKC.

Results and discussion

MDCK cells robustly form polarized cysts when grown in reconstituted basement membrane (Matrigel) and provide a good system in which to screen for morphogenesis defects (Martín-Belmonte et al., 2007). However, no canine shRNA libraries are currently available. Therefore, to screen for GEF function, we constructed a library of 70 shRNAs in pSUPER against the canine Rho family GEFs for which sequences were available in GenBank (Table S2). These plasmids were individually nucleofected into MDCK cells, which were then plated onto Matrigel pads, as described previously (Martín-Belmonte et al., 2007). After 4 d, the cells had formed cysts, which were stained with phalloidin and examined by fluorescence microscopy (Fig. 1). 70–75% of the control cysts had single lumens under our growth conditions. Phalloidin highlights actin that is highly enriched at the apical cortex, thereby marking the central lumen. Lumen morphology was scored in triplicate wells (>100 cysts/well) for each shRNA and normalized to the control, for which cells were transfected with an shRNA against luciferase (Fig. 1 A). Many shRNAs had no effect on lumen formation, but six shRNAs consistently caused significant perturbations in lumen formation (>30% decrease in single lumens). These shRNAs targeted *Tuba*, *intersectin 2* (*ITSN2*), *SGEF*, *p114 Rho GEF*, *LBC*, and *AlsCL* (Fig. 1, A and B). To determine whether these shRNAs were disrupting lumen formation through off-target effects, we constructed new shRNAs against different regions of the same genes (Table S1) and retested them. In each case, the same phenotype was observed, arguing that these were bona fide hits against genes required for normal cyst morphogenesis.

We focused on Tuba because it is specific for Cdc42 and has been implicated previously in tight junction organization (Otani et al., 2006). However, ITSN2 is also a Cdc42 GEF, raising the possibility that the observed effects might be nonspecific results of a global decrease in Cdc42-GTP that could occur after depletion of any GEF for this GTPase. Indeed, Cdc42 depletion causes a multilumen phenotype in MDCK cells (Martín-Belmonte et al., 2007). To address this issue, we checked the other known Cdc42-specific GEFs that were negative in our screen. ASEF and FGD1 were not detectably expressed in MDCK cells by RT-PCR. However, Zizimin/Dock 9 was detectable, and expression was significantly reduced by the shRNA used in the screen (Fig. S1 A). Moreover, the overexpression of GFP-Zizimin did not rescue the lumen defect caused by loss of Tuba (Fig. S1 B). ITSN2 also did not rescue lumen formation (Fig. S1 C). Therefore, we conclude that Tuba performs specific functions during cyst formation that cannot be compensated by the overexpression of a different Cdc42 GEF.

Tuba is a large protein (~180 kD), the C-terminal half of which contains two SH3 domains and a Bar domain, in addition to the DH (Dbl homology) domain that catalyzes guanine nucleotide exchange (Salazar et al., 2003). The N terminus contains multiple SH3 domains that bind dynamin. Tuba is expressed as several variants, the smallest of which lacks the dynamin-binding domain. Immunoblotting confirmed that our two shRNAs silenced expression of all detected variants by >70% (Fig. 2 A), a value similar to the transfection efficiency obtained using nucleofection in MDCK cells. Both shRNAs produced defects in cyst morphogenesis to a degree that correlated with the level of silencing (Fig. 2, A and B).

To confirm that the lumen defect resulting from transfection with *Tuba* shRNAs was caused by loss of Tuba protein, we performed a rescue experiment. Endogenous Tuba was first stably silenced by infection with a *Tuba*-shRNA lentivirus (Table S1). After 72 h, the cells were nucleofected with a human full-length GFP-Tuba fusion, and 24 h later, the cells were plated onto Matrigel and grown as cysts for a further 48 h. Human Tuba (hTuba), which is not recognized by our shRNAs against the canine gene, was able to fully rescue normal cyst morphogenesis (Fig. 2 B). In addition, to test whether the GEF activity of Tuba is important for lumen formation, we deleted the DH domain from GFP-hTuba. This mutant did not efficiently rescue cyst morphogenesis (Fig. 2 B), so we conclude that Tuba Cdc42 GEF activity is required for this process. Interestingly, the DH deletion mutant produced lumen defects even in a wild-type background, indicating that it behaves as a dominant negative (Fig. 2 C).

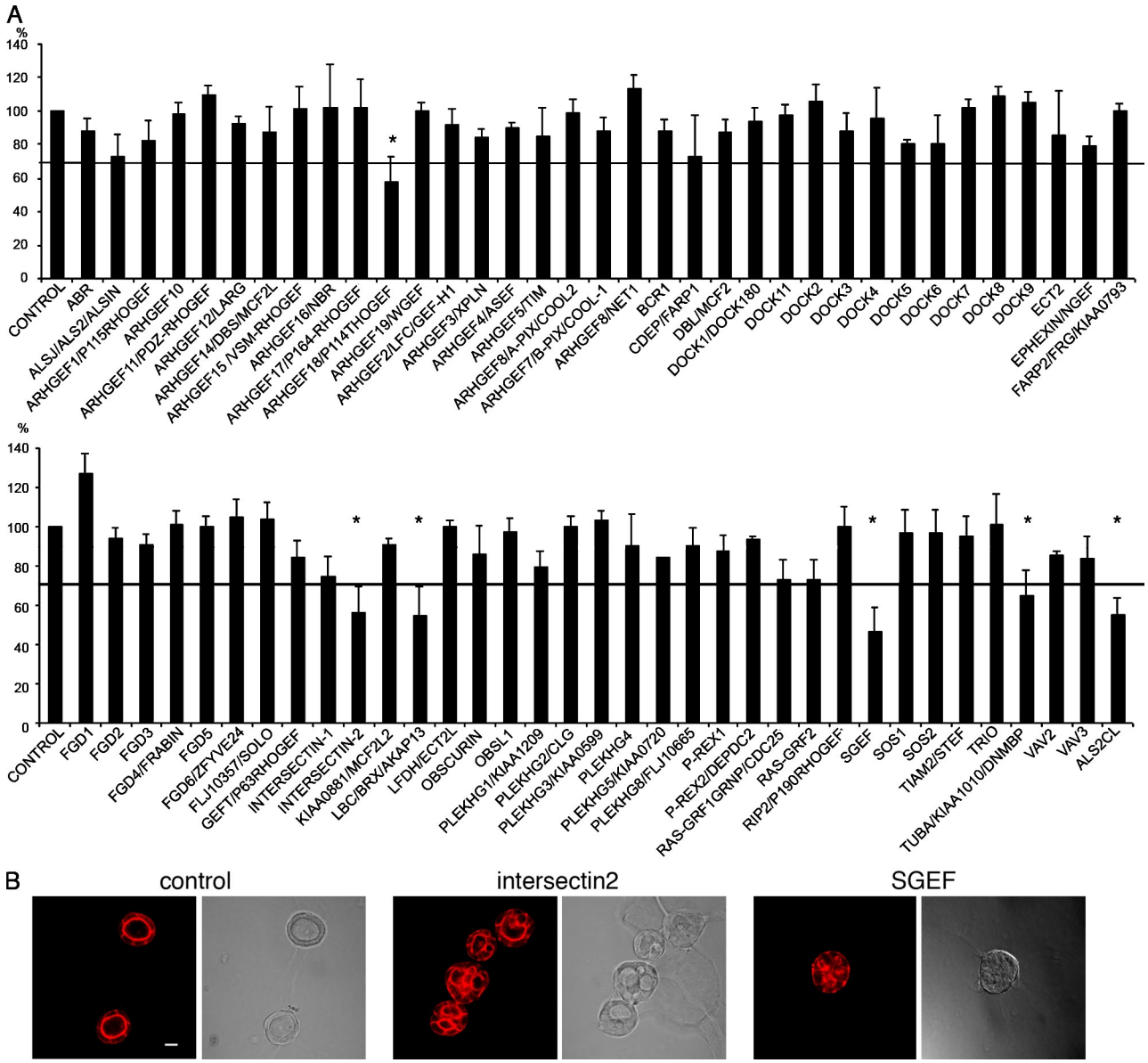

Figure 1. **RNAi screen for Rho GEFs involved in lumen formation.** (A) pSUPER vectors expressing shRNAs against canine Rho GEFs were nucleofected into MDCK cells. After 18 h, cells were transferred to Matrigel and incubated for 3 d. Cysts stained with phalloidin were scored for single central lumens (n > 100 scored in triplicate for each shRNA, and compared with the control, which was normalized to 100%). Error bars indicate ±1 SD (n = 3). Horizontal lines show the cut-off of 70%, which was used to select putative hits. Asterisks mark GEFs that, when silenced by shRNA, reduced normal lumen formation by >30%. (B) Examples of cyst defects showing differential interference contrast images and actin staining. Bar, 20 µm.

This result is consistent with an important role for the DH domain of Tuba in lumen formation.

Because GFP-hTuba is functional, we used this construct to determine its distribution in MDCK cells. Available antibodies against Tuba did not enable specific staining of cysts. Tuba in Caco-2 cell monolayers is enriched at tight junctions and binds ZO-1 (Otani et al., 2006), but this localization is cell line specific and does not occur in MDCK monolayers where Tuba is mostly cytoplasmic (unpublished data). Notably, in cysts, we found that GFP-Tuba is concentrated subapically (Fig. 3 A). It does not colocalize with either gp135/podocalyxin, an apical transmembrane protein (Meder et al., 2005), or with ZO-1, a marker of tight junctions, but resides above the nuclei close to the apical cortex. Thus, Tuba might specifically activate Cdc42 in the apical region of the cell. To test this possibility, we asked whether we could detect a change in Cdc42 localization in response to the loss of Tuba. Because there are no antibodies available to detect endogenous Cdc42 by immunofluorescence, we used a stable cell line that expresses a GFP-Cdc42 fusion protein at close to endogenous levels and that has been validated by Martín-Belmonte et al. (2007). GFP-Cdc42 is diffuse throughout the cytoplasm but is significantly enriched at the apical cortex of MDCK cell cysts, coincident with podocalyxin (Fig. 3, B and C). Strikingly, depletion of Tuba abolishes this apical enrichment, which is consistent with the idea that Tuba controls apical Cdc42 activation (Fig. 3 C).

Based on the requirement for GEF activity by Tuba to rescue cyst morphogenesis, we would predict that silencing of Tuba

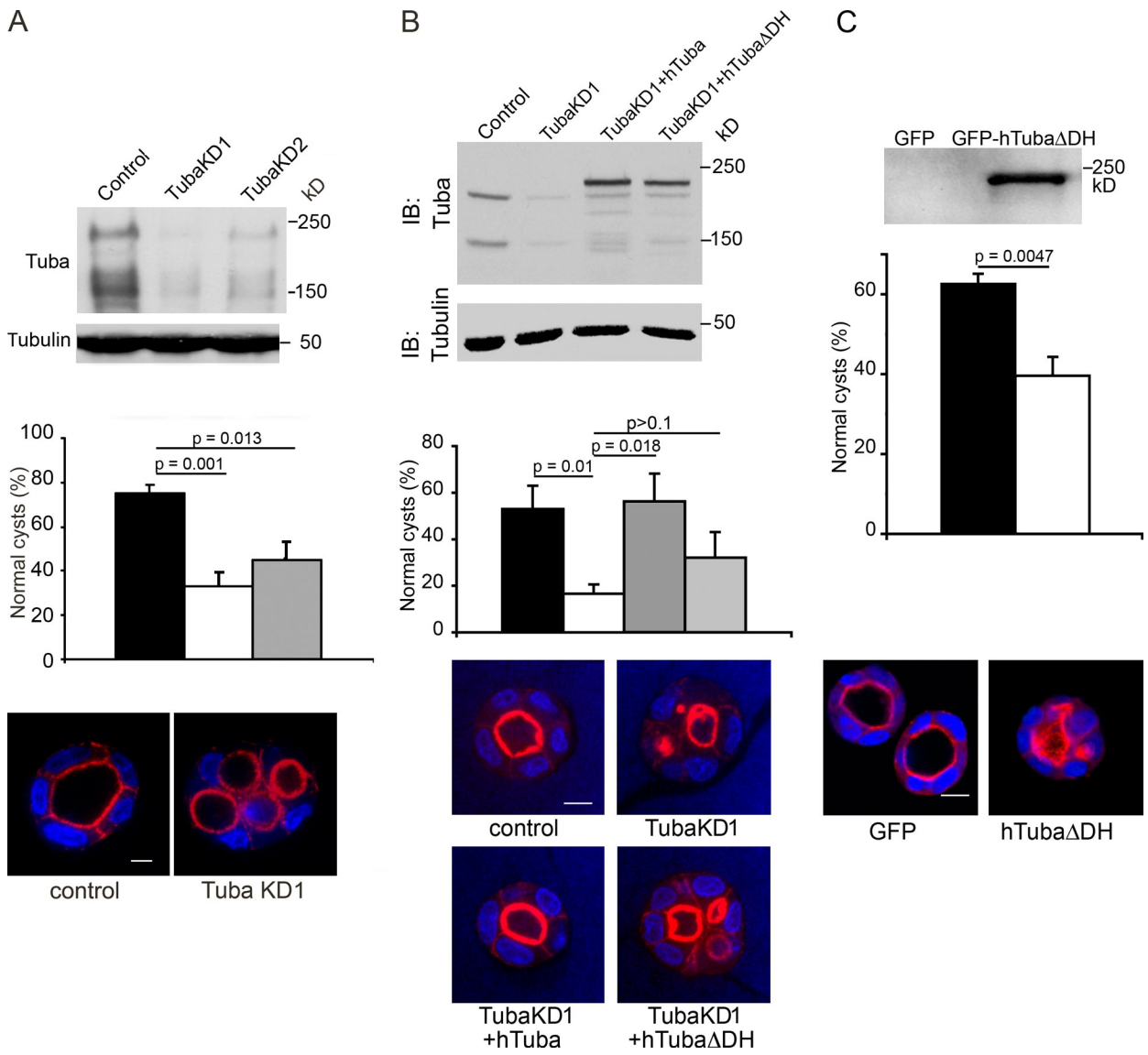

Figure 2. **Silencing Tuba causes defective lumen formation that can be rescued by intact but not GEF-defective hTuba.** (A) Immunoblot of Tuba from lysates of cells transfected with shRNAs against luciferase or canine Tuba. Tubulin was a loading control. Cysts were scored for normal lumens. (B) Immunoblot (IB) showing lentivirus-mediated silencing of Tuba and expression of full length GFP-hTuba fusion or a mutant lacking the catalytic DH domain. Bottom panels show representative confocal images of cysts after growth in Matrigel for 48 h. (C) Effect of GFP-Tuba lacking the DH domain on lumen formation. Cells were nucleofected with GFP alone or the mutant Tuba and scored for multiple lumens after growth in Matrigel for 48 h. Values are means ± 1 SD (n = 3; >100 cysts counted per experiment); p-values were calculated using an unpaired t test. Cysts were stained for actin and for DNA, and representative images are shown. Histograms show percentages of cysts with single lumens. Bars, 10 µm.

expression might reduce cellular Cdc42-GTP. However, if production of the GTP-bound form is highly localized, no overall reduction might be detectable. Indeed, pull-down assays using the PAK (p21-activated kinase)-binding domain to capture Cdc42-GTP were unable to detect any reproducible difference in control versus Tuba-depleted cells (unpublished data). Therefore, we asked whether we could rescue lumen formation by expressing a gain of function Cdc42 mutant in the context of the TubaKD shRNA. Cdc42(Q61L) rescued cyst morphogenesis almost as efficiently as the GFP-hTuba fusion (Fig. 3 D), which is consistent with the argument that the multilumen phenotype is caused by reduced Cdc42-GTP.

If Tuba regulates lumen formation via the activation of a pool of Cdc42, depletion of Cdc42 from cells might cause a similar phenotype to loss of Tuba. Indeed, Martín-Belmonte et al. (2007) have reported that siRNAs against Cdc42 cause a multilumen phenotype in MDCK cells. To confirm this observation, we tested three shRNAs for knockdown of the canine *Cdc42* (Fig. 4 A). One of these, Cdc42KD2, was inserted into a lentivirus and transduced into cells that were then plated on Matrigel. This shRNA caused a severe defect in cyst morphogenesis (Fig. 4 B). In Caco-2 cells, multilumen formation caused by loss of Cdc42 has been ascribed to misorientation of the mitotic spindle (Jaffe et al., 2008). To determine whether a similar mechanism occurs in MDCK cells, we transduced the cells with lentiviruses targeting Cdc42 or Tuba and plated them immediately into Matrigel so cysts would form before knockdown. Using this method, most of the cysts still contained only a single

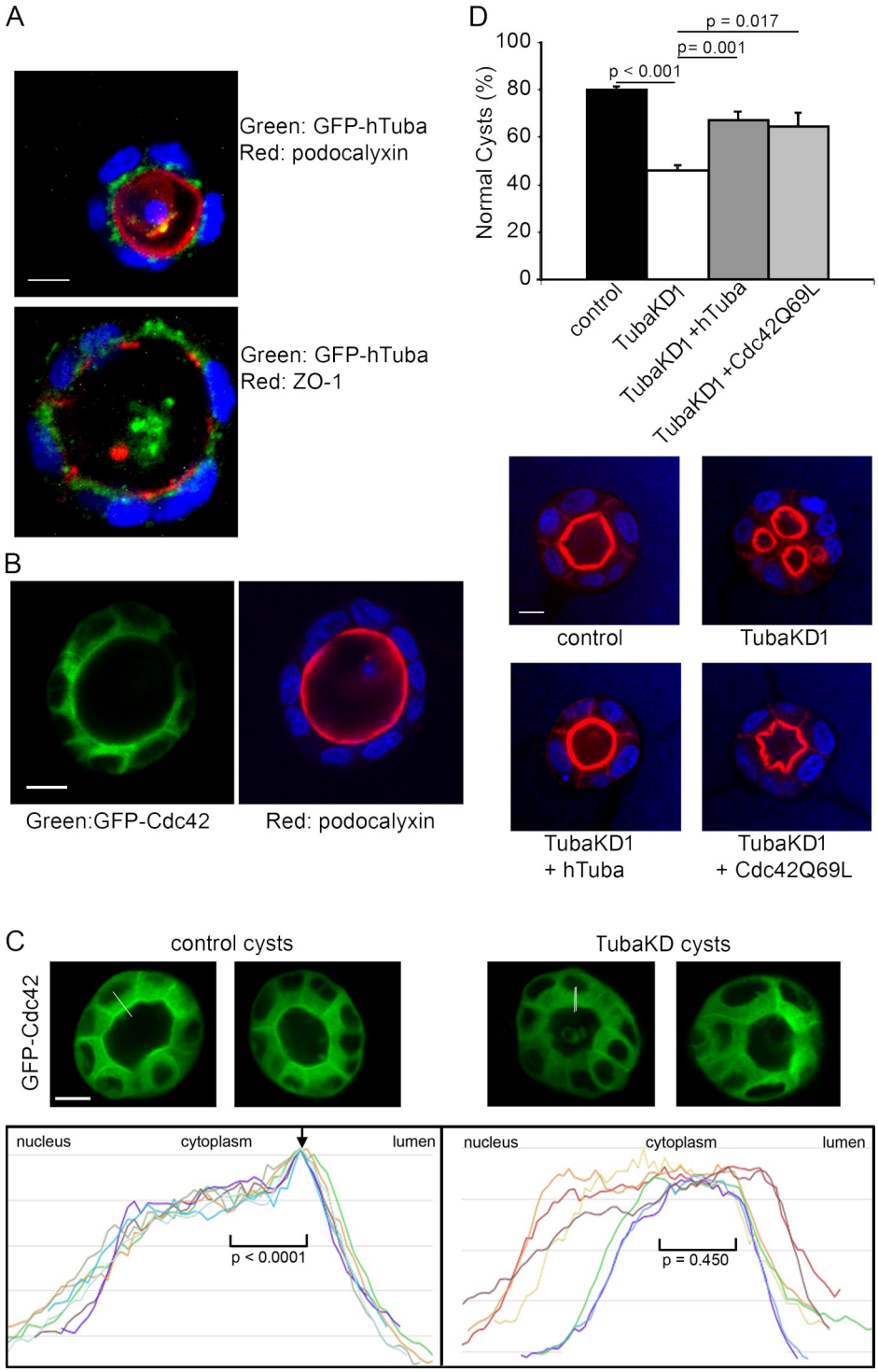

Figure 3. **Localization of GFP-Tuba and -Cdc42 and rescue of lumen formation by an activated Cdc42.** (A) Confocal images of cysts expressing GFP-hTuba. Cysts were fixed and stained for GFP plus either gp135/podocalyxin or ZO-1 and DNA. (B) Cysts stably expressing GFP-Cdc42. Cysts were fixed and stained for GFP plus podocalyxin. (C) Live cell imaging of cells that stably express GFP-Cdc42, showing loss of apical enrichment after silencing of Tuba. Bottom panels show profiles across lines drawn from the nucleus to the lumen ($n = 7$ cysts each). Intensity differences between cortex and cytoplasm were compared using a paired two-tailed *t* test. Each color in the plots represents a different cell from different lysates. The arrow indicates the position of the apical cortex. (D) Cells were nucleofected with pSUPER-luciferase or pSUPER-TubaKD ± vectors expressing GFP-hTuba or a constitutively active mutant of Cdc42. Cysts were fixed at 72 h and then scored and analyzed as in Fig. 2. Bottom panels show representative confocal sections stained for actin and DNA. Bars, 10 µm.

lumen when examined after 3 d, and spindle orientation could be measured accurately with respect to the plane of the cyst surface. As expected, in control cysts, virtually all mitoses occurred in the plane of the cyst surface (mean angle 11.3 ± 2.2° SEM; Fig. 4 C). Cdc42 silencing completely randomized spindle orientation (mean angle 44 ± 4.5° SEM), as was reported for Caco-2

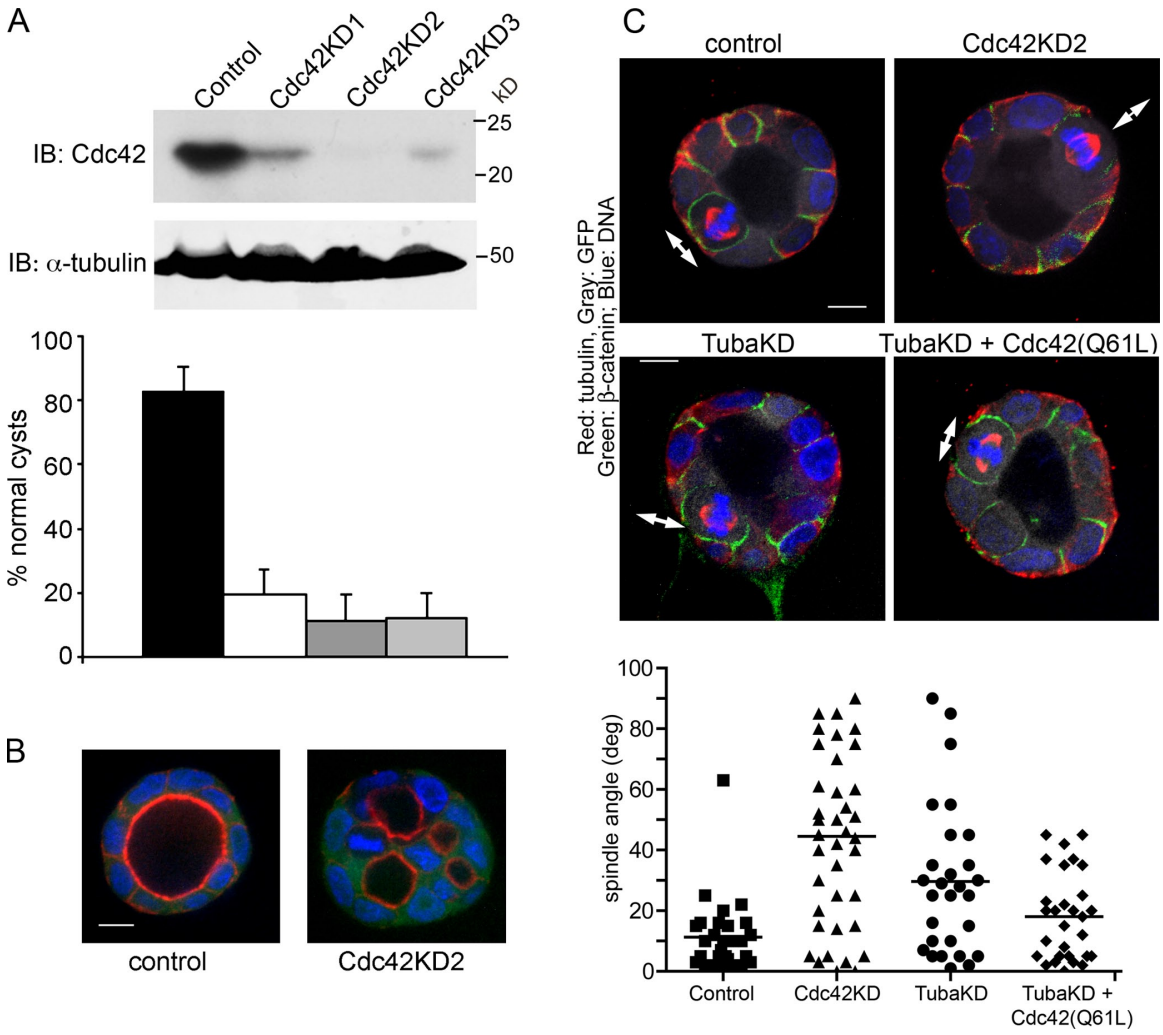

Figure 4. **Silencing of either Tuba or Cdc42 randomizes the mitotic spindle orientation in MDCK cysts.** (A) Immunoblot (IB) showing silencing of Cdc42 by different shRNAs. Tubulin was used as a loading control. The histogram shows the percentage of cysts with single lumens for each shRNA ($n > 100$; error bars are ±1 SD). (B) Representative confocal slices through normal and Cdc42-depleted cysts. (C) Misorientation of spindles caused by depletion of Tuba or Cdc42. Cells were infected with lentiviruses that express shRNAs against luciferase (control), Tuba, or Cdc42 and then immediately plated into Matrigel and grown as cysts for 3.5 d. After staining for DNA, tubulin, β-catenin, and GFP, mitotic cells were analyzed for the spindle angle with respect to the basal surface. Representative images show the orientation of mitosis in control and Cdc42- or Tuba-depleted cells. Arrows indicate the orientation of the mitotic spindles. Quantification of spindle angles is shown on the bottom. Median angle for each condition is shown as a line. An angle of zero was ascribed to mitoses that occurred in the exact plane of the cyst surface (parallel to the basal cortex). deg, degree. Bars, 10 µm.

cells (Jaffe et al., 2008), whereas loss of Tuba also caused significant spindle misorientation, although to a lesser extent (mean angle 30 ± 4.5° SEM). Importantly, the Cdc42(Q61L) mutant also rescued normal spindle orientation in the Cdc42-depleted cysts (mean angle 18 ± 2.7° SEM), which is consistent with the idea that multilumen formation is indeed a consequence of defective spindle orientation and that Cdc4 activation plays a role in orientation (Fig. 4 C). These data illuminate a simple mechanism whereby loss of Tuba could result in multiple lumen formation within the cysts.

Cdc42-GTP can bind to Par6 and relieve an inhibitory constraint on aPKC activity (Yamanaka et al., 2001; Atwood et al., 2007), and aPKC activity has been shown previously to be required for normal lumen organization in MDCK cell cysts (Martín-Belmonte et al., 2007). Therefore, we asked whether Tuba functions to regulate aPKC activity. Phosphorylation of Thr410 has been used as a measure of aPKC activity (Standaert et al., 2001), and blotting with an antibody against this phosphorylated site revealed that, as expected, depletion of Cdc42 caused a significant decrease in phospho-Thr410 (Fig. 5 A). Notably, a significant decrease was also observed in cells depleted of Tuba (Fig. 5 B). In addition, consistent with experiments using cells from conditional Cdc42 knockout mice (Wu et al., 2007), the Ser9 phosphorylation of GSK-3β, a putative aPKC target, was reduced after expression of shRNAs against either Cdc42 or Tuba. Importantly, aPKC localization at the apical cortex was not abolished by depletion of Tuba, arguing that, in epithelial cells, Cdc42-GTP does not function in the recruitment of Par6–aPKC as was reported for astrocytes (Etienne-Manneville and Hall, 2001; note that, as described in the previous paragraph, cells were plated into Matrigel immediately after lentiviral transduction, so silencing would not take effect until cysts had already formed; Fig. 5 C). We conclude that Tuba is required to produce Cdc42-GTP, which stimulates apical aPKC, which in turn

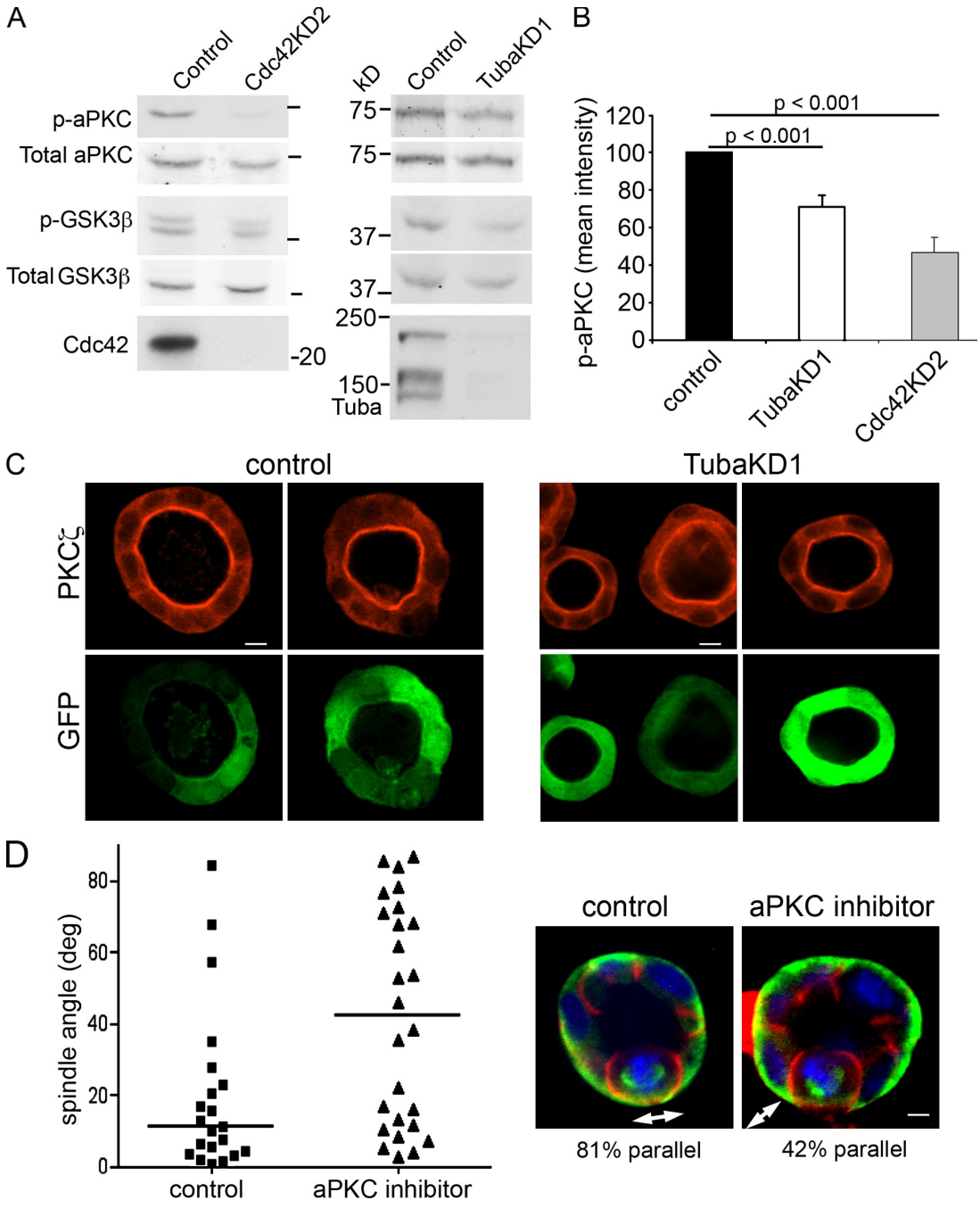

Figure 5. **Silencing of Tuba or Cdc42 reduces Thr410 aPKC phosphorylation and GSK-3β phosphorylation on Ser9 but does not cause mislocalization of aPKC from the apical surface.** (A) MDCK cells were transduced with lentiviruses expressing shRNAs against Cdc42 or Tuba. After 3–4 d in monolayer culture, the cells were grown as cysts in Matrigel for a further 3 d. Cells were harvested and immunoblotted for total aPKC and GSK-3β or the phosphoproteins as shown. Band intensities were measured either using an Odyssey system or by scanning. (B) The histogram shows mean band intensities for an immunoblot of aPKC phospho-Thr410 ± 1 SEM (n = 3 for Tuba and 7 for Cdc42). P-values were calculated using the Wilcoxon signed-rank test. (C) Cells were infected with lentivirus and then immediately plated into Matrigel, as for Fig. 4 C, so that cysts would form before the knockdown had taken effect. Cysts were fixed and stained for GFP (green), as a marker for lentiviral transduction, and for endogenous aPKC (red) 3 d after transduction. (D) Inhibition of aPKC randomizes spindle pole orientation. Cysts were treated for 24 h with 40 µM myristoylated pseudosubstrate peptide, and after incubation for 24 h, they were fixed and stained for α-tubulin (green), β-catenin (red), and DNA (blue). Arrows indicate the orientation of the mitotic spindles. Orientations were measured as in Fig. 4. Horizontal bars show the median. Significance of difference was tested using a two-tailed t test with unequal variance ($P = 0.0065$). deg, degree. Bars, 10 µm.

controls spindle orientation during cyst morphogenesis. Silencing of aPKC is toxic to cells, so to test whether aPKC activity is necessary for spindle orientation, we used a myristoylated pseudosubstrate for the kinase, which specifically inhibits aPKC. As predicted, this inhibitor caused a significant spindle orientation defect ($P < 0.01$; Fig. 5 D).

The polarity proteins Par6 and aPKC play important roles in epithelial organization, and Cdc42-GTP has been proposed

to recruit Par6 to the apical surface of MDCK epithelial cells through an indirect association with annexin2 (Martín-Belmonte et al., 2007). However, it remains unclear whether Cdc42 can bind simultaneously to annexin and Par6. Par6 is also recruited directly to the apical surface through interactions with Pals1 and/or Crumbs, which bind the Par6 PDZ (PSD95/DLGA/ZO-1) domain. Interaction with Pals1 is stimulated by Cdc42-GTP (Hurd et al., 2003), which provides a simple mechanism to promote Par6–aPKC apical enrichment and activity. A pivotal unanswered question concerned how Cdc42 is activated at the apical cortex. Our screen identified Tuba as a Cdc42-specific GEF required for normal spindle orientation and for full aPKC activation. Tuba is localized appropriately for such a function, near the apical cortex. The mechanism of localization is unknown, but it is tempting to speculate that Tuba associates with phosphoinositides in the apical membrane via its Bar domain. The Tuba phenotype was less dramatic than that caused by depletion of Cdc42, but the efficiency of Tuba knockdown was less than that of Cdc42. In addition, it is conceivable that Tuba is partially redundant with other Cdc42 GEFs. However, as discussed above (Fig. 1 and Fig. S1), Cdc42-specific GEFs other than ITSN2 either had no effect on lumen formation (Zizimin) or were not detectably expressed in MDCK cells.

Finally, a key goal is to identify the mechanism downstream of Cdc42–Par6–aPKC that controls spindle orientation in mammalian epithelial cells. One attractive possibility is that the attachment of astral microtubules to the cell cortex is blocked at the apical surface by aPKC activity, which might phosphorylate and remove an attachment factor. Potential factors include murine Pins (Du and Macara, 2004), the dynein subunit LIC2 (Schmoranzer et al., 2009), and the microtubule plus end–binding protein APC (adenomatous polyposis coli; Yamashita et al., 2003), all of which have been implicated in signaling downstream of the Par proteins.

Materials and methods

Materials

Anti–α-tubulin was obtained from Sigma-Aldrich, Alexa Fluor 546–phalloidin was purchased from Invitrogen, anti–PKC-ζ was obtained from Santa Cruz Biotechnology, Inc., and Alexa Fluor 488, 546, and 633 were purchased from Invitrogen. For immunoblotting, antibodies for phospho–GSK-3β (Ser9) and phospho–PKC-λ/ζ were obtained from Cell Signaling Technology, and GSK-3β, PKC-λ, β-catenin, and Cdc42 were purchased from BD. Anti-GFP antibody was obtained from Abcam. HRP-conjugated secondary antibodies were obtained from Jackson ImmunoResearch Laboratories, Inc., Alexa Fluor 680 was purchased from Invitrogen, and IRDye 800 was purchased from Rockland Immunochemicals, Inc. Monoclonal antibody to podocalyxin/gp135 was a gift from G. Ojakian (State University of New York Downstate Medical Center, Brooklyn, NY). Polyclonal anti-Tuba antibodies and HA-tagged Tuba plasmid were provided by P. de Camilli (Yale University, New Haven, CT). Myristoylated PKC-ζ pseudosubstrate was obtained from Invitrogen. The Tuba ORF was subcloned into pBluescript II vector and then moved into pK-GFP using XbaI and HindIII sites. To create GFPΔDH, the full-length GFP-Tuba vector was cut with BglII and HpaI, which deleted the DH domain sites, and religated with a linker to maintain the correct frame. The pLVTHM lentivector and packaging system (psPAX2, pMD2.G) were provided by D. Trono (École Polytechnique Fédérale de Lausanne, Lausanne, Switzerland). The GFP-Zizimin vector was a gift from M. Schwartz (University of Virginia, Charlottesville, VA). ITSN2 was provided by S. de la Luna (Institució Catalana de Recerca i Estudis Avançats and Centre de Regulació Genòmica, Barcelona, Spain), and the GFP-Cdc42 MDCK line was provided by F. Martín-Belmonte (Centro de Biología Molecular Severo Ochoa, Madrid, Spain).

RNAi screen

74 shRNA complementary DNA strands against canine GEFs (Table S1) were grouped into six subpools, annealed, phosphorylated, ligated into the BglII and HindIII sites of GFP-pSUPER, and transformed into XLI-Blue. Individual transformants were sequenced, and plasmids were purified from those containing the correct sequences. 70 of these pSUPER-shRNA plasmids were then nucleofected into MDCK-T23 cells, using 2 µg per 2 million cells (Chen and Macara, 2005). Transfection efficiency was estimated using the GFP marker. After overnight culture, cells were plated onto solid Matrigel and grown in MEM with 5% fetal bovine serum plus 2% Matrigel (O'Brien et al., 2001) in 8-well slides (Lab Tek II; Thermo Fisher Scientific) in triplicate. Each well contained 1.5×10^4 cells. After 3 d, cysts were fixed, stained with phalloidin, and analyzed by fluorescence microscopy. Cysts with single central lumens were counted as normal.

Tuba and Cdc42 shRNAs

The following sequences were used: TubaKD1, 5′-GGAAATATGCAGATGGTGA-3′; TubaKD2, 5′-GCAGAGAAGTTAAAGGACA-3′; Cdc42KD1, 5′-GCAAGAGGATTAGACAGA-3′; Cdc42KD2, 5′-GATTACGACCGCTGAGTTA-3′; and Cdc42KD3, 5′-GCGATGGTGCCGTTGGTAA-3′ with appropriate flanking sequences. The annealed, phosphorylated oligonucleotides were ligated into pSUPER or pLVTHM. pSUPER constructs were transfected into cells, and cysts were formed as described in the previous section. Silencing was determined by immunoblotting 4 d after transfection. For stable suppression, lentivirus was produced as described previously, using a second generation packaging system (McCaffrey and Macara, 2009). Silencing was determined by immunoblotting 3 and 7 d after infection.

Microscopy

For immunofluorescence staining, the cysts were washed in PBS then fixed in 4% paraformaldehyde, washed, and then permeabilized with 0.25% Triton X-100 for 10 min (O'Brien et al., 2001). After blocking with 0.7% gelatin and 0.1% saponin, the cysts were incubated with the required antibodies in PBS overnight at 4°C. Secondary antibodies coupled with Alexa Fluor 488, 546, or 633 were incubated with the fixed specimens for 2–3 h at room temperature. Cysts were mounted in Prolong Gold antifade reagent (Invitrogen) and imaged at room temperature on a microscope (Eclipse TE2000-E; Nikon) with a Yokogawa spinning disk confocal system (Solamere Technologies, Inc.) using a 60× NA 1.40 oil-immersion objective lens, and a camera (iCCD; Stanford Photonics). The acquisition software used was InVivo (Media Cybernetics). In the initial screen, we used a microscope (510 LSM Meta; Carl Zeiss, Inc.) with a 20× NA 0.4 objective lens, using the manufacturer's software. Images were processed using Volocity (PerkinElmer) and assembled using Photoshop 7.0 (Adobe).

Immunoblotting

Cells in Matrigel or monolayer cultures were washed gently with PBS, lysed in 4× Laemmli sample buffer, and boiled for 10 min. After resolution on SDS-PAGE and blotting onto nitrocellulose, proteins were incubated with primary antibodies overnight at 4°C. Signals were detected with either ECL (Thermo Fisher Scientific) and quantified by scanning or were analyzed using an infrared imager (Odyssey; LI-COR Biosciences). Statistical analysis was performed using the Wilcoxon signed-rank test.

Measurement of mitotic spindle angle

To measure the spindle angle, cells were plated on Matrigel immediately after lentiviral infection. Cysts were allowed to form for 3.5 d before fixation. Using this approach, most of the cysts still contained only a single lumen. Confocal images of cysts containing cells in metaphase were collected. Only those mitotic cells that were GFP positive and in which both spindle poles were in the same focal plane were selected for analysis. Spindle angle was measured relative to the plane of the basal surface. Those spindles exactly parallel to the basal cell surface were ascribed an angle of 0°. Statistical analysis was performed using an unpaired *t* test.

Online supplemental material

Fig. S1 shows that Zizimin is a Cdc42 GEF that does not regulate lumen formation in MDCK cells. Table S1 contains additional sequences selected in a secondary screen to confirm putative hits. Table S2, included as an Excel file, contains GenBank accession numbers, selected sequences, and shRNA oligonucleotides used for the Rho GEF screen. Online supplemental material is available at http://www.jcb.org/cgi/content/full/jcb.201002097/DC1.

We thank Didier Trono, Martin Schwartz, Pietro de Camilli, Susana de la Luna, and Fernando Martín-Belmonte for reagents and other members of the Macara laboratory for helpful suggestions.

This work was supported in part by grant GM070902 from the National Institutes of Health and by the James and Rebecca Craig Foundation.

Submitted: 17 February 2010
Accepted: 16 April 2010

Note added in proof. In this issue, Rodriguez-Fraticelli et al. (2010. *J. Cell Biol.* doi:10.1083/jcb.201002047) describe a role for another Cdc42 GEF, ITSN2, in spindle pole orientation during epithelial cyst formation.

References

Aceto, D., M. Beers, and K.J. Kemphues. 2006. Interaction of PAR-6 with CDC-42 is required for maintenance but not establishment of PAR asymmetry in *C. elegans*. *Dev. Biol.* 299:386–397. doi:10.1016/j.ydbio.2006.08.002

Anderson, D.C., J.S. Gill, R.M. Cinalli, and J. Nance. 2008. Polarization of the *C. elegans* embryo by RhoGAP-mediated exclusion of PAR-6 from cell contacts. *Science*. 320:1771–1774. doi:10.1126/science.1156063

Atwood, S.X., C. Chabu, R.R. Penkert, C.Q. Doe, and K.E. Prehoda. 2007. Cdc42 acts downstream of Bazooka to regulate neuroblast polarity through Par-6 aPKC. *J. Cell Sci.* 120:3200–3206. doi:10.1242/jcs.014902

Casamayor, A., and M. Snyder. 2002. Bud-site selection and cell polarity in budding yeast. *Curr. Opin. Microbiol.* 5:179–186. doi:10.1016/S1369-5274(02)00300-4

Chen, X., and I.G. Macara. 2005. Par-3 controls tight junction assembly through the Rac exchange factor Tiam1. *Nat. Cell Biol.* 7:262–269. doi:10.1038/ncb1226

Du, Q., and I.G. Macara. 2004. Mammalian Pins is a conformational switch that links NuMA to heterotrimeric G proteins. *Cell*. 119:503–516. doi:10.1016/j.cell.2004.10.028

Etienne-Manneville, S., and A. Hall. 2001. Integrin-mediated activation of Cdc42 controls cell polarity in migrating astrocytes through PKCzeta. *Cell*. 106:489–498. doi:10.1016/S0092-8674(01)00471-8

Garrard, S.M., C.T. Capaldo, L. Gao, M.K. Rosen, I.G. Macara, and D.R. Tomchick. 2003. Structure of Cdc42 in a complex with the GTPase-binding domain of the cell polarity protein, Par6. *EMBO J.* 22:1125–1133. doi:10.1093/emboj/cdg110

Hurd, T.W., L. Gao, M.H. Roh, I.G. Macara, and B. Margolis. 2003. Direct interaction of two polarity complexes implicated in epithelial tight junction assembly. *Nat. Cell Biol.* 5:137–142. doi:10.1038/ncb923

Hutterer, A., J. Betschinger, M. Petronczki, and J.A. Knoblich. 2004. Sequential roles of Cdc42, Par-6, aPKC, and Lgl in the establishment of epithelial polarity during *Drosophila* embryogenesis. *Dev. Cell*. 6:845–854. doi:10.1016/j.devcel.2004.05.003

Jaffe, A.B., N. Kaji, J. Durgan, and A. Hall. 2008. Cdc42 controls spindle orientation to position the apical surface during epithelial morphogenesis. *J. Cell Biol.* 183:625–633. doi:10.1083/jcb.200807121

Joberty, G., C. Petersen, L. Gao, and I.G. Macara. 2000. The cell-polarity protein Par6 links Par3 and atypical protein kinase C to Cdc42. *Nat. Cell Biol.* 2:531–539. doi:10.1038/35019573

Lin, D., A.S. Edwards, J.P. Fawcett, G. Mbamalu, J.D. Scott, and T. Pawson. 2000. A mammalian PAR-3-PAR-6 complex implicated in Cdc42/Rac1 and aPKC signalling and cell polarity. *Nat. Cell Biol.* 2:540–547. doi:10.1038/35019592

Martín-Belmonte, F., A. Gassama, A. Datta, W. Yu, U. Rescher, V. Gerke, and K. Mostov. 2007. PTEN-mediated apical segregation of phosphoinositides controls epithelial morphogenesis through Cdc42. *Cell*. 128:383–397. doi:10.1016/j.cell.2006.11.051

McCaffrey, L.M., and I.G. Macara. 2009. The Par3/aPKC interaction is essential for end bud remodeling and progenitor differentiation during mammary gland morphogenesis. *Genes Dev.* 23:1450–1460. doi:10.1101/gad.1795909

Meder, D., A. Shevchenko, K. Simons, and J. Füllekrug. 2005. Gp135/podocalyxin and NHERF-2 participate in the formation of a preapical domain during polarization of MDCK cells. *J. Cell Biol.* 168:303–313. doi:10.1083/jcb.200407072

Motegi, F., and A. Sugimoto. 2006. Sequential functioning of the ECT-2 RhoGEF, RHO-1 and CDC-42 establishes cell polarity in *Caenorhabditis elegans* embryos. *Nat. Cell Biol.* 8:978–985. doi:10.1038/ncb1459

O'Brien, L.E., T.S. Jou, A.L. Pollack, Q. Zhang, S.H. Hansen, P. Yurchenco, and K.E. Mostov. 2001. Rac1 orientates epithelial apical polarity through effects on basolateral laminin assembly. *Nat. Cell Biol.* 3:831–838. doi:10.1038/ncb0901-831

Otani, T., T. Ichii, S. Aono, and M. Takeichi. 2006. Cdc42 GEF Tuba regulates the junctional configuration of simple epithelial cells. *J. Cell Biol.* 175:135–146. doi:10.1083/jcb.200605012

Salazar, M.A., A.V. Kwiatkowski, L. Pellegrini, G. Cestra, M.H. Butler, K.L. Rossman, D.M. Serna, J. Sondek, F.B. Gertler, and P. De Camilli. 2003. Tuba, a novel protein containing bin/amphiphysin/Rvs and Dbl homology domains, links dynamin to regulation of the actin cytoskeleton. *J. Biol. Chem.* 278:49031–49043. doi:10.1074/jbc.M308104200

Schmoranzer, J., J.P. Fawcett, M. Segura, S. Tan, R.B. Vallee, T. Pawson, and G.G. Gundersen. 2009. Par3 and dynein associate to regulate local microtubule dynamics and centrosome orientation during migration. *Curr. Biol.* 19:1065–1074. doi:10.1016/j.cub.2009.05.065

Schonegg, S., and A.A. Hyman. 2006. CDC-42 and RHO-1 coordinate acto-myosin contractility and PAR protein localization during polarity establishment in *C. elegans* embryos. *Development*. 133:3507–3516. doi:10.1242/dev.02527

Standaert, M.L., G. Bandyopadhyay, Y. Kanoh, M.P. Sajan, and R.V. Farese. 2001. Insulin and PIP3 activate PKC-zeta by mechanisms that are both dependent and independent of phosphorylation of activation loop (T410) and autophosphorylation (T560) sites. *Biochemistry*. 40:249–255. doi:10.1021/bi0018234

Welchman, D.P., L.D. Mathies, and J. Ahringer. 2007. Similar requirements for CDC-42 and the PAR-3/PAR-6/PKC-3 complex in diverse cell types. *Dev. Biol.* 305:347–357. doi:10.1016/j.ydbio.2007.02.022

Wells, C.D., J.P. Fawcett, A. Traweger, Y. Yamanaka, M. Goudreault, K. Elder, S. Kulkarni, G. Gish, C. Virag, C. Lim, et al. 2006. A Rich1/Amot complex regulates the Cdc42 GTPase and apical-polarity proteins in epithelial cells. *Cell*. 125:535–548. doi:10.1016/j.cell.2006.02.045

Wu, X., S. Li, A. Chrostek-Grashoff, A. Czuchra, H. Meyer, P.D. Yurchenco, and C. Brakebusch. 2007. Cdc42 is crucial for the establishment of epithelial polarity during early mammalian development. *Dev. Dyn.* 236:2767–2778. doi:10.1002/dvdy.21309

Yamanaka, T., Y. Horikoshi, A. Suzuki, Y. Sugiyama, K. Kitamura, R. Maniwa, Y. Nagai, A. Yamashita, T. Hirose, H. Ishikawa, and S. Ohno. 2001. PAR-6 regulates aPKC activity in a novel way and mediates cell-cell contact-induced formation of the epithelial junctional complex. *Genes Cells*. 6:721–731. doi:10.1046/j.1365-2443.2001.00453.x

Yamashita, Y.M., D.L. Jones, and M.T. Fuller. 2003. Orientation of asymmetric stem cell division by the APC tumor suppressor and centrosome. *Science*. 301:1547–1550. doi:10.1126/science.1087795